Biomedicine & Pharmacotherapy 160 (2023) 114369

Contents lists available at ScienceDirect

Biomedicine & Pharmacotherapy

journal homepage: www.elsevier.com/locate/biopha

Toward model-informed precision dosing for tamoxifen: A population-pharmacokinetic model with a continuous CYP2D6 activity scale

Bram C. Agema [a,b,*], Sanne M. Buijs [a], Sebastiaan D.T. Sassen [b,c], Thomas E. Mürdter [d,e], Mathias Schwab [d,f,g], Birgit C.P. Koch [b,c], Agnes Jager [a], Ron H.N. van Schaik [h], Ron H. J. Mathijssen [a], Stijn L.W. Koolen [a,b]

[a] Dept. of Medical Oncology, Erasmus MC Cancer Institute, Erasmus University Medical Center; Rotterdam, the Netherlands
[b] Dept. of Clinical Pharmacy, Erasmus University Medical Center; Rotterdam, the Netherlands
[c] Rotterdam Clinical Pharmacometrics Group; Rotterdam, the Netherlands
[d] Margarete Fischer-Bosch-Institute of Clinical Pharmacology; Stuttgart, Germany
[e] University of Tübingen; Tübingen, Germany
[f] Dept. of Clinical Pharmacology, University Hospital Tübingen; Tübingen, Germany
[g] iFIT Cluster of Excellence (EXC2180) "Image Guided and Functionally Instructed Tumor Therapies", University of Tübingen, Tübingen, Germany
[h] Dept. of Clinical Chemistry, Erasmus University Medical Center, Rotterdam, the Netherlands

ARTICLE INFO

Keywords:
Tamoxifen
Endoxifen
CYP2D6
Pharmacokinetics
Pharmacometrics
Model-informed precision dosing (MIPD)

ABSTRACT

Background: Tamoxifen is important in the adjuvant treatment of breast cancer. A plasma concentration of the active metabolite endoxifen of $\geq$ 16 nM is associated with a lower risk of breast cancer-recurrence. Since inter-individual variability is high and > 20 % of patients do not reach endoxifen levels $\geq$ 16 nM with the standard dose tamoxifen, therapeutic drug monitoring is advised. However, ideally, the correct tamoxifen dose should be known prior to start of therapy. Our aim is to develop a population pharmacokinetic (POP-PK) model incorporating a continuous CYP2D6 activity scale to support model informed precision dosing (MIPD) of tamoxifen to determine the optimal tamoxifen starting dose.

Methods: Data from eight different clinical studies were pooled (539 patients, 3661 samples) and used to develop a POP-PK model. In this model, CYP2D6 activity per allele was estimated on a continuous scale. After inclusion of covariates, the model was subsequently validated using an independent external dataset (378 patients). Thereafter, dosing cut-off values for MIPD were determined.

Results: A joint tamoxifen/endoxifen POP-PK model was developed describing the endoxifen formation rate. Using a continuous CYP2D6 activity scale, variability in predicting endoxifen levels was decreased by 37 % compared to using standard *CYP2D6* genotype predicted phenotyping. After external validation and determination of dosing cut-off points, MIPD could reduce the proportion of patients with subtherapeutic endoxifen levels at from 22.1 % toward 4.8 %.

Conclusion: Implementing MIPD from the start of tamoxifen treatment with this POP-PK model can reduce the proportion of patients with subtherapeutic endoxifen levels at steady-state to less than 5 %.

1. Introduction

Tamoxifen is being used for decades to prevent disease recurrence and mortality in patients suffering from estrogen receptor-positive breast cancer. In prior research, five years of adjuvant tamoxifen therapy reduced breast cancer recurrence with 42 % and breast cancer specific death by 22 % [1]. However, despite this effective treatment, breast cancer still recurred in 30 % of patients within 15 years of follow-up [2,3].

Tamoxifen is a prodrug which is metabolized by CYP2D6 and CYP3A4 into 4-hydroxytamoxifen, N-desmethyl-tamoxifen and is subsequently metabolized into its most clinically relevant metabolite;

* Correspondence to: Erasmus MC Cancer Institute, Erasmus University Medical Center, Dr. Molewaterplein 40, 3015 GD Rotterdam, the Netherlands.
E-mail address: b.agema@erasmusmc.nl (B.C. Agema).

https://doi.org/10.1016/j.biopha.2023.114369
Received 11 January 2023; Received in revised form 1 February 2023; Accepted 3 February 2023
Available online 6 February 2023

endoxifen [4]. Endoxifen competes with estrogen for the estrogen receptor and thereby inhibits the stimulating effect of estrogen on breast cancer cells [5]. An exposure – response relationship of endoxifen was found in a large retrospective cohort and an activity threshold of 16 nM endoxifen plasma concentration was reported [6]. Patients with endoxifen levels below this threshold showed 26 % higher breast cancer recurrence rates compared to patients with endoxifen levels above the 16 nM threshold. The endoxifen exposure – response relation has been validated in a different study showing that patients with endoxifen concentrations < 14 nM had an almost two-fold higher risk of distant recurrence [7]. Therefore, it is hypothesized that applying therapeutic drug monitoring (TDM) of tamoxifen to verify that patients are above the 16 nM endoxifen threshold could further decrease disease recurrence.

A large cohort study showed that approximately 21 % of patients did not reach sufficient steady-state endoxifen levels (<16 nM), using the standard dose of 20 mg tamoxifen once daily. When TDM was applied, the proportion of patients below the threshold was reduced to 11 % [8]. However, as endoxifen reaches steady-state after three months, six months was needed to assign the correct personalized dose to each patient. Ideally, the appropriate dose to reach the endoxifen threshold concentration should be known prior to starting tamoxifen treatment. If the appropriate dose is not known, patients could be exposed to insufficient endoxifen levels and thus, suboptimal treatment. Selecting the optimal dose, from the start of treatment, using model-informed precision dosing (MIPD) may solve these problems.

To date, six population pharmacokinetic (pop-PK) models have been developed to describe both tamoxifen and endoxifen PK [9–14]. These models found that inter-individual variation (IIV) on the rate of endoxifen formation was best explained by *CYP2D6* phenotype or CYP2D6 activity score with scores of 0, 0.5 or 1 per allele. However, recent findings showed that CYP2D6 activity could also be described on a more sensitive continuous scale [15]. In this study we use a continuous CYP2D6 activity scale to develop a more sensitive pop-PK model. This model may, in turn, be used in MIPD to treat the patient with the correct tamoxifen dose when starting tamoxifen treatment.

2. Materials and methods

2.1. Clinical database

Data was pooled from multiple datasets originating from eight different clinical studies conducted in the Erasmus Medical Center Cancer Institute. Both, sparse data describing tamoxifen/endoxifen PK over multiple years and dense data describing PK during a single-dose interval were available. Sparse PK data was provided by the TOTAM study, a prospective open-label intervention study [8]. Female patients treated with adjuvant tamoxifen for breast cancer were eligible for participation. In this study, blood samples were obtained from patients at 3, 4.5, 6, 12, 18 and 24 months after starting tamoxifen treatment. Dense PK data was available from seven studies which were studying possible interacting agents (*i.e.* rifampicin, curcumin, green tea, probenecid, and cannabidiols) [16–20], the effect of circadian rhythm on tamoxifen PK [21], or using dextromethorphan as phenotyping test to predict endoxifen plasma concentrations [22]. All PK samples which were taken during co-administration with a potent interacting agent were excluded to ensure model and covariate stability. In total, 37 participants of the mentioned dense sampling studies also participated in the TOTAM study. All patients provided written informed consent prior to participation and all studies were conducted according to the declaration of Helsinki.

All PK samples in the clinical database were analyzed in the laboratory of translational pharmacology at the Erasmus MC Cancer Institute using a validated LC-MS/MS method [23]. *CYP2D6* and *CYP3A4* genotyping analyses were performed using both the Quantstudio (ThermoFisher Scientific; Waltham, MA) and the Infiniti (Autogenomics; Carlsbad, CA) machines.

2.2. Population PK model

All PK data was converted into molar values and subsequently logarithmically transformed prior to modeling. Initially, tamoxifen PK data was modeled to a one-compartmental model with first order absorption and first order elimination. Thereafter, multi-compartmental models, different absorption models (lag-time, transit compartments, Weibull absorption, and zero-order absorption), different elimination models (zero-order, nonlinear clearance) and introduction of exponentially modeled IIV, on different parameters were tested. Subsequently, the available NDM-tamoxifen and 4-hydroxytamoxifen samples were added to the model. Thereafter, endoxifen was included in the model using a first-order metabolic rate with IIV. Residual error in plasma concentrations was estimated with a proportional error model. As two types of data were available, the residual error was separately estimated for each data type (*i.e.* dense, sparse) and each compound. In addition, for the dense data, inter-occasional variability (IOV) was introduced to account for differences between dense sampling occasions.

The effect of *CYP2D6* genotype on the endoxifen formation rate was incorporated as a continuous scale into the model. When an allele was present in less than two patients, the activity score was fixed to the categorical activity score of Pharmvar (activity of 0, 0.5 or 1) [24]. If the *CYP2D6* genotype was unknown, the genotype was assigned to a distinct variable for unknown CYP2D6 activity so that known alleles were not affected by this group. The allele showing the lowest activity expressed by at least five patients was fixed to 0 (no activity) and the * 1 genotype was fixed to 1 (full activity). An additional parameter estimated the relative amount of the formation rate to be dependent of *CYP2D6* genotype activity. All patients in the model development dataset were tested for *CYP2D6* * 1 - * 7, * 9, * 10, * 17, * 29, * 31, * 41 and duplications.

To further explain variability in the endoxifen formation rate, weight, height, age, body mass index (BMI), lean body mass (LBM), and body surface area (BSA) were tested as continuous covariates. These were centered on the median and tested as power models. Missing values were replaced by the carry-forward method or if no data was known the median value was imputed. *CYP3A4 * 22* genotype and radiation therapy were tested as categorical covariates. Covariates models were included using a stepwise forward inclusion ($p < 0.05$) with backward elimination ($p < 0.01$) procedure.

2.3. Model validation

The final model was internally evaluated using visual predictive checks (VPCs). External validation was performed using data from the Margarete Fischer-Bosch-Institute of Clinical Pharmacology in Stuttgart, Germany [25]. Patient characteristics of this population are depicted in the Appendix. In contrast to the model-development dataset, patients were not screened for harboring *CYP2D6* * 2 (normal activity), * 17 (decreased activity), * 29 (decreased activity) or * 31 (no activity) alleles, whereas patients in the validation set were screened for the * 35 allele (normal activity), which was not present in the model development dataset. These patients were excluded from the validation. Using the final model the median prediction error (MDPE) (<20 %), the median absolute prediction error (MAPE) (<30 %), and the fraction within 30 % ($F_{30\%}$) (>50 %) and 20 % ($F_{20\%}$) (>35 %) were calculated to test the accuracy and precision of the final model [26,27].

2.4. MIPD simulations

Cut-off values for each dosing interval (20, 30 or 40 mg) were determined using receiver operating characteristic (ROC) curves. The population prediction was used as a predictor whereas the first measured endoxifen trough concentration at steady-state was used as

true value. The optimal cut-off point was determined, as proposed by Perkins and Schisterman, using the prevalence of subtherapeutic endoxifen concentrations in the dataset and a cost which was set to 0.35 in consultation with clinicians [28]. After determining the cut-off points, this dosing strategy was implemented on both the development dataset as well as the validation dataset.

3. Results

3.1. Clinical database

The model-development dataset constituted of 539 patients and 3613 plasma samples in which both endoxifen and tamoxifen were quantified. Almost half of these samples were steady-state trough levels (n = 1655), whereas the other half (n = 1958) constituted of dense PK data from one of 165 24 h-cycles on steady-state. In total, data from 25 patients and 11 additional samples were excluded due to concomitant CYP2D6 inhibitor use (12 patients), missing dosing information (seven patients), tamoxifen non-adherence (six patients and three additional samples) or samples that were accidentally taken after discontinuation of tamoxifen therapy (six samples), two samples were excluded as both the tamoxifen and endoxifen concentrations from a patient raised by 50 % after hospitalization for allopurinol induced drug induced rash with eosinophilia and systemic symptoms. The endoxifen and tamoxifen concentrations thereafter returned to normal steady-state concentrations. Patient characteristics are depicted in Table 1. All patients were treated in the adjuvant setting for primary breast cancer (stage I to stage III breast cancer). Patient characteristics per study population and the validation dataset are shown in table S1.

Table 1
Patient characteristics of the model-development cohort.

Patient characteristic	*Median*	*IQR*
Age (years)	56	47–65
Height (cm)	168	164–173
Weight (kg)	74	66–84
BMI (kg/m^2)	26.1	23.0–29.9
BSA (m^2)	1.87	1.75–1.99
LBM (kg)	45.3	41.9–49.1
Data type		
Dense	134	24.4 %
Sparse	415	75.6 %
	No.	*%*
CYP2D6 alleles		
*1/*2	83	15.1 %
*1/*4	76	13.8 %
*1/*1	72	13.1 %
*1/*41	36	6.6 %
*2/*2	33	6.0 %
*2/*41	30	5.5 %
*2/*4	28	5.1 %
*4/*4	22	4.0 %
*1/*9	15	2.7 %
*1/*5	11	2.0 %
*4/*41	10	1.8 %
*4/*5	8	1.5 %
*2/*5	8	1.5 %
*2/*3	8	1.5 %
*2/*9	7	1.3 %
*1/*10	7	1.3 %
*4/*10	6	1.1 %
Unknown	10	1.8 %
Other	123	13.5 %
CYP3A4 alleles		
*1/*1	366	66.7 %
*1/*22	16	2.9 %
*22/*22	4	0.7 %
Unknown	163	29.7 %

BMI, body mass index; BSA, body surface area; IQR, inter-quartile range; LBM, lean body mass.

3.2. Population PK model

The final model is schematically presented in Fig. 1. A two-compartmental model with an additive error model best described simultaneous tamoxifen and endoxifen plasma concentrations. As NDM-tamoxifen and 4-hydroxytamoxifen were quantified in only 37 % of all samples, inclusion of these samples introduced significant instability and high shrinkage to the model and were therefore excluded. In the base model, IIV was modeled on tamoxifen clearance and the transformation rate of tamoxifen to endoxifen. Endoxifen distribution volume was fixed to 400 L as reported earlier in literature and also used in previous models describing tamoxifen/endoxifen PK [10,29]. Absorption was best described by a combined an absorption lag time followed by first order absorption. The addition of a peripheral tamoxifen compartment introduced model instability and was hence discarded. For endoxifen, the additional compartment did not lead to a significantly improved model. The clearance of both endoxifen and tamoxifen was best described by a first-order rate. Introduction of IOV on tamoxifen clearance or endoxifen formation rate between different 24-hour cycles introduced a shrinkage > 30 % and was therefore not incorporated into the final structural model.

The influence of *CYP2D6* genotype on endoxifen formation rate was modeled on a continuous scale and multiplied by a parameter estimating the percentage of the endoxifen formation rate to be CYP2D6 dependent. Duplicate fully active (*1 and *2) alleles were pooled as the CYP2D6 activity score predictions were similar. Inclusion of CYP2D6 phenotypes decreased the inter-individual variability (IIV) of the endoxifen formation rate from 59.0 % to 42.8 %. Inclusion of known CYP2D6 activity score subgroups instead of phenotypes decreased the IIV from 59.0 % to 33.4 % and a model-predicted continuous CYP2D6 activity scale decreased the IIV further to 26.8 %. After careful evaluation of the residual unexplained IIV a power term was added to the equation ensuring a good fit over all values of CYP2D6 activity, which decreased unexplained IIV by 0.6 % (Eq. 1) (Fig. S1).

$$CYP2D6activity = (Allele_1 + Allele_2/2)^{\theta} \quad (1)$$

In this equation, *Allele1* and *Allele2* represent the activity of each allele. θ is the exponent which was estimated by NONMEM (Table 2).

Model-predicted CYP2D6 activity scores of the most common allele combinations are depicted in Table 2. A visual comparison of the categorical phenotyping scale, the gene activity score [30], and the model-estimated activity scale, of CYP2D6 is shown in Fig. 2.

In addition to *CYP2D6* genotype, patients' BMI significantly

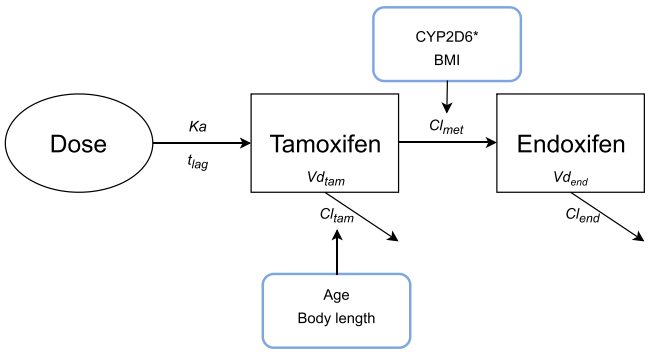

Fig. 1. Schematic representation of the final population PK model structure and the incorporated covariate relationships represented in the blue boxes. * The influence of CYP2D6 on the endoxifen formation rate was modeled as seen in Eq. 1. Ka, absorption rate; t_{lag}, lag time; Vd_{tam}, apparent distribution volume of tamoxifen. Cl_{tam}, apparent clearance of tamoxifen; Cl_{met}, apparent endoxifen formation rate; BMI, body mass index; Vd_{end}, apparent distribution volume of endoxifen. Cl_{end}, apparent clearance of endoxifen. (For interpretation of the references to color in this figure legend, the reader is referred to the web version of this article.)

Table 2
Final model parameter estimates.

Parameter	*Estimate*	*95 % CI*	*Shrinkage*
K_a (h)	1.45	1.13–1.77	
t_{lag} (h)	0.44	0.37–0.50	
Vd_{tam}/F (L)	880	729–1031	
Cl_{tam}/F (L/h)	7.38	7.18–7.58	
Cl_{met}/F (L/h)	0.155	0.113–0.197	
Vd_{end}/F (L)	400	FIX	
Cl_{end}/F (L/h)	1.23	0.91–1.56	
CYP2D6 alleles			
*1	1.000	FIX	
*2	0.560	0.476–0.644	
*3	0.066	0.024–0.108	
*4	0.047	0.018–0.076	
*5	0.040	0.007–0.073	
*6	0.000	FIX	
*7	0.000	FIX	
*9	0.378	0.267–0.489	
*10	0.103	0.028–0.178	
*17	0.156	0.064–0.248	
*29	0.490	0.278–0.702	
*31	0.000	FIX	
*41	0.110	0.052–0.168	
duplicate *1/*2	1.400	0.806–1.994	
Unknown	0.589	0.369–0.809	
Exponent (Eq. 1)	0.606	0.466–0.746	
% CYP2D6 mediated*	0.946	0.892–1.000	
Covariates			
Age (Cl_{tam})†	-0.414	-0.535 to −0.293	
Patient height (Cl_{tam})†	1.460	0.670– 2.250	
BMI (Cl_{met}) †	-0.394	-0.511 to −0.277	
Additive error model			
Dense data			
Tamoxifen	0.153	0.143–0.161	3.1 %
Endoxifen	0.161	0.151– 0.171	3.1 %
Sparse data			
Tamoxifen	0.188	0.178–0.198	11.0 %
Endoxifen	0.186	0.177–0.195	11.4 %
Residual IIV			
IIV Cl_{tam}	32.0 %		3.7 %
IIV Cl_{met}	25.3 %		11.0 %

*This parameter estimated the percentage of the endoxifen formation rate to be CYP2D6 dependent. † Power model. ‡ Proportional model.
Ka, absorption rate; t_{lag}, lag time; Vd_{tam}, apparent distribution volume of tamoxifen; Cl_{tam}, apparent clearance of tamoxifen; Cl_{met}, apparent endoxifen formation rate; BMI, body mass index; Vd_{end}, apparent distribution volume of endoxifen; Cl_{end}, apparent clearance of endoxifen; FIX, parameter was not estimated but set to this value.

influenced the endoxifen formation rate. Including these covariates in the model, diminished unexplained variability in the endoxifen formation rate from 26.8 % to 25.1 %. Tamoxifen clearance was influenced by both age and patient height. Inclusion of these covariates reduced IIV on this parameter from 34.7 % to 32.1 %. CYP3A4 * 22 genotype, radiation therapy, LBM, BSA and weight did not affect endoxifen or tamoxifen PK to a significant extent. The effect of each covariate on the steady-state endoxifen concentrations is shown in Fig. 3. All parameter estimates and their corresponding 95 % confidence intervals and shrinkages are depicted in Table 2.

3.3. Model validation

Six patients were excluded from the external validation dataset as these patients harbored a CYP2D6 allele which was not present in the model-development dataset. As patient height was missing in 61 % of cases, it was imputed in the validation dataset when missing, using a reference dataset from the Dutch central bureau for statistics which contained the estimated height for each age group depending on their birth year [31]. External model validation showed that the model adequately described the data by meeting the criteria mentioned in the methods section (MDPE, −1.53 %; MAPE, 34.25 %; F_{20}, 39.06 %; F_{30}, 55.21 %).

3.4. MIPD simulations

Dosing cut-off points were determined using ROC curves (Fig. S2). The optimal cut-off point was determined with prevalence set to 23 % and cost set to 0.35. The cut-off point for receiving 40 mg tamoxifen was a model-predicted steady-state level of 11.40 nM endoxifen when treated with 20 mg tamoxifen. When the model predicted that a patient will not reach 20.23 nM endoxifen at steady-state when using 20 mg tamoxifen, this patient should be given 30 mg. Patients with a predicted endoxifen concentration above 20.23 nM will be treated with the standard dose of 20 mg. Simulations showed that instead of 22.1 % not reaching sufficient endoxifen levels, using these model-informed dosing recommendations could diminish this proportion to 9.9 %. When also switching patients that were identified to be at risk for not being capable of reaching endoxifen thresholds even at the maximum registered dose of 40 mg (steady state endoxifen $<$ 8.56 nM), to aromatase inhibitors, the proportion of patients that does not reach 16 nM endoxifen decreases further toward 4.8 %. The results of imposing this dosing strategy on the first endoxifen samples in the model development dataset is visualized in Fig. 4A. Out of all patients with a simulated dose-increase, 19.7 % showed endoxifen plasma concentrations $>$ 32 nM and could have been treated with a lower dose. In addition, from all patients which were recommended to be switched, 30.0 % could manage to obtain endoxifen plasma levels $>$ 16 nM with 40 mg.

When imposing these dosing cut-off points on the external validation set, a similar reduction in patients with endoxifen plasma concentrations $<$ 16 nM is seen. Whereas with a one-dose-fits-all dosing regimen 17.9 % of patients do not reach endoxifen levels $>$ 16 nM, with MIPD this could be reduced to 9.5 % (Fig. 4B) and further toward 6.5 % when also switching patients at risk for underexposure on 40 mg to aromatase inhibitors.

4. Discussion

Using a continuous individual CYP2D6 allele activity score, the model's accuracy to predict endoxifen trough concentrations was significantly improved compared to using CYP2D6 phenotypes. Therefore using this model for MIPD could reduce the number of patients being below the threshold of 16 nM from 22.1 % toward 4.8 % immediately after reaching steady-state. Similar results were seen when simulating the MIPD in an external dataset. The addition of MIPD using this model at the start of tamoxifen treatment could help to ensure a fast and safe determination of the right tamoxifen dose.

Continuous-scale CYP2D6 activity assignment has been previously performed in one study [15]. The assignments of our predicted activity scores per genotype using NONMEM are comparable to this study. However, in this previous research, an additive model with an addition from a neural network when a patient harbored a single * 1 genotype was used. As no machine learning was implemented in this research, we described the relation between genotypes and CYP2D6 activity using a power model.

Although most of the IIV was explained, 25 % still remains unexplained. This could be due to patients harboring SNPs which were not included in our panel. However, the minor allele frequency of these are low (<1 %) or, like *CYP2D6 * 35,* are known to minimally affect CYP2D6 activity compared to a fully functioning variant [24]. Therefore, we feel this should not significantly affect the results of our activity scale. Besides, non-genetic causes such as treatment adherence, which was not quantified in every dataset, or unknown interactions are more likely explaining this residual variability.

In addition to the more sensitive CYP2D6 activity scale, age and patient height affected tamoxifen clearance, whereas BMI influenced endoxifen formation rate. Although age has been described in previous tamoxifen models [10], patient height has not been described as an

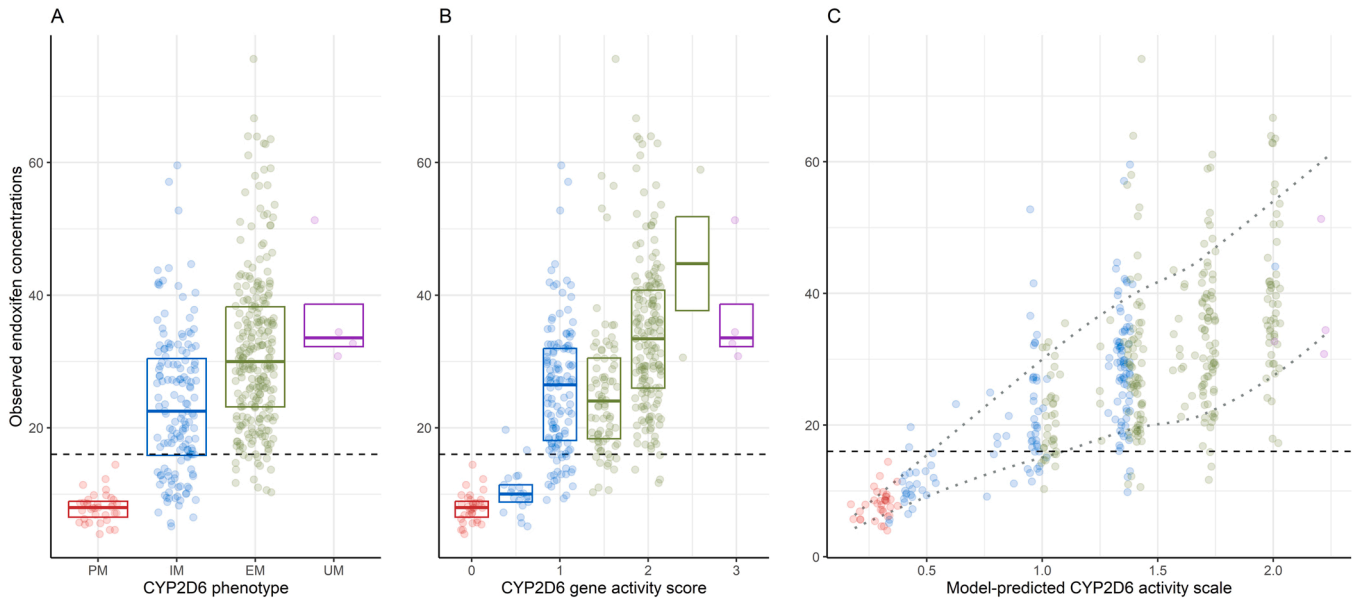

Fig. 2. Comparison of conventional and the model-predicted CYP2D6 activity scales. The observed endoxifen concentration was stratified on conventional CYP2D6 predicted phenotype (A), gene activity score (B) and the model-predicted CYP2D6 activity score (C). Data comprised of the first endoxifen trough observations at steady-state. The dotted lines represent the interval in which 80% of all datapoints lie. The dashed horizontal line represents the 16 nM effectivity threshold. The colors represent the predicted phenotype where red dots represent poor metabolizers, blue represents the intermediate metabolizers, green represents the extensive metabolizers and purple dots represent ultrarapid metabolizers. PM, poor metabolizer; IM, intermediate metabolizer; EM, extensive metabolizer; UM, ultrarapid metabolizer. (For interpretation of the references to color in this figure legend, the reader is referred to the web version of this article.)

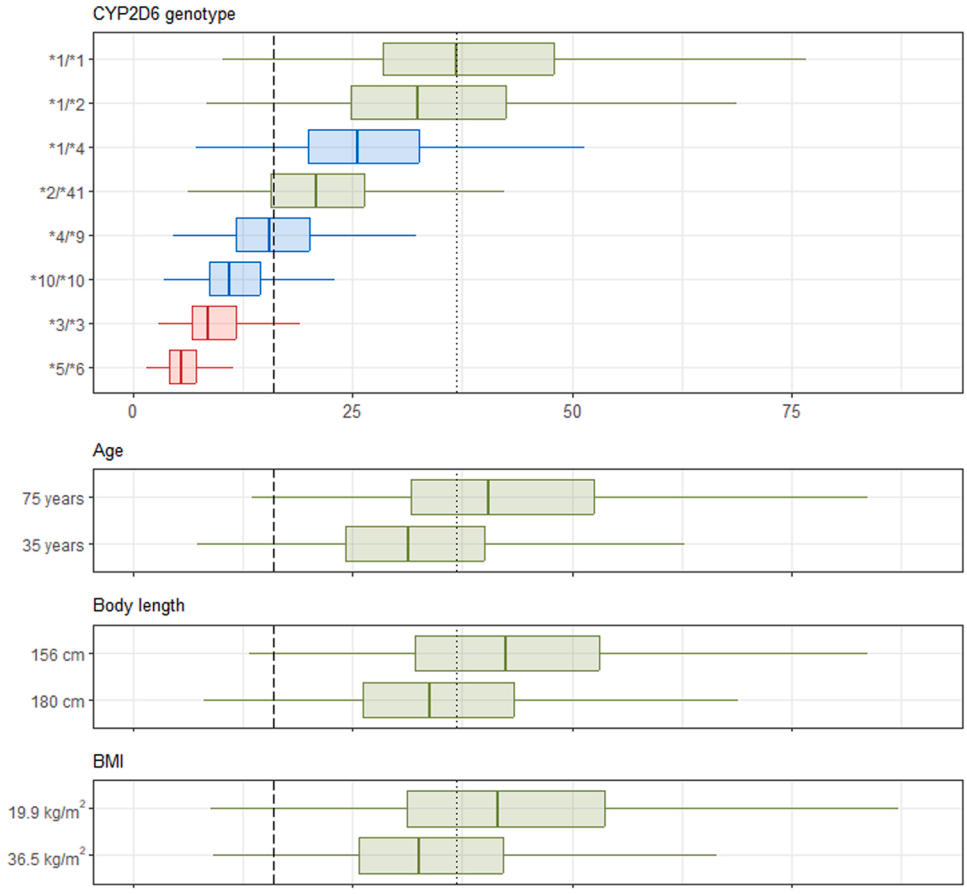

Fig. 3. Effect of incorporated covariates on the predicted steady-state endoxifen concentration. For every situation, 1000 simulations were run. For CYP2D6, different genotypes were depicted based on prevalence and activity score. In the CYP2D6 simulations, other covariates were set to the median. In the other simulations, the * 1/* 1 genotype was used. CYP2D6 phenotypes are represented by colors where red is poor metabolizer, blue is intermediate metabolizer, and green represents normal/extensive metabolizer. The 16 nM threshold is shown as a dashed-line. The dotted line represents the median of a person with median age (56 years), patient height (168 cm), BMI (26.03 kg/m^2) and a * 1/* 1 genotype. BMI, body mass index. (For interpretation of the references to color in this figure legend, the reader is referred to the web version of this article.)

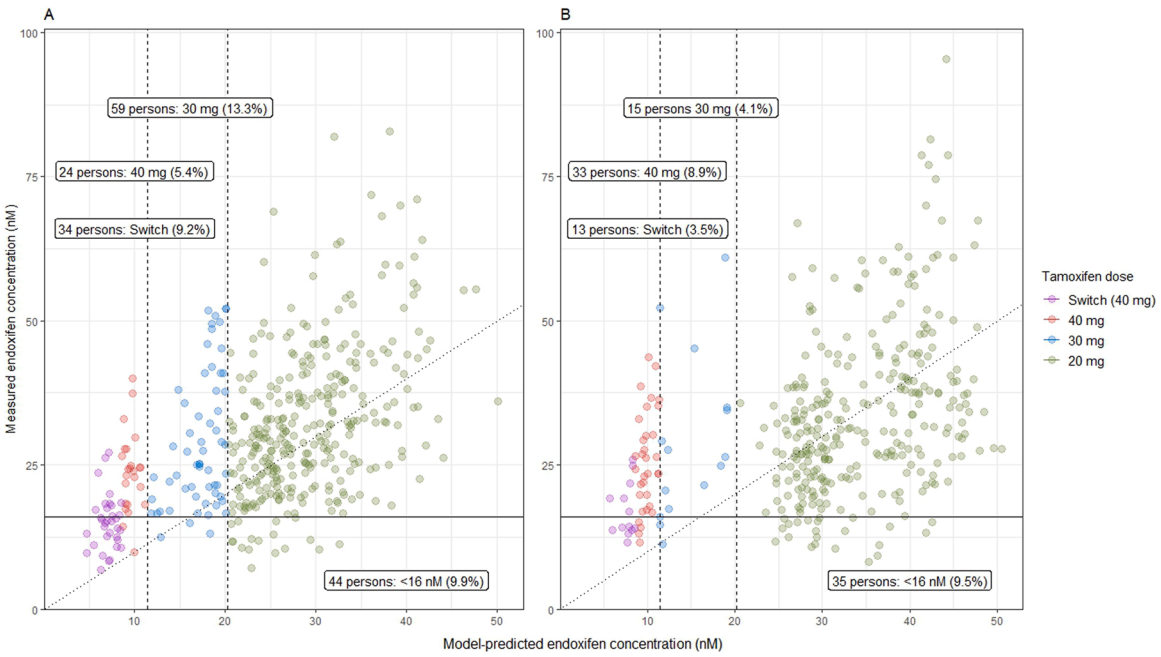

Fig. 4. Simulation of model-informed prediction dosing for tamoxifen/endoxifen. (A) Data comprised of the first endoxifen trough concentrations at steady-state in patients in the model development dataset (n = 443). (B) The MIPD cut-off points simulated in the external dataset (n = 369). The horizontal line represents the 16 nM effectivity threshold and the vertical lines represent the 40 mg and the 30 mg dosing cut-off values. The dotted line is the unity line.

influential covariate. However, as IIV was only modeled on tamoxifen clearance, patient height may be affecting distribution volume as tamoxifen is mostly distributed into organs, which size are affected by patient height [32]. The effect of BMI or body weight has already been described in previous papers [9,10,33]. As BMI is mostly affected by body weight instead of height and the covariate analysis was performed using forward inclusion, including both in the model is feasible.

Because the validation cohort was not specifically tailored for this study some covariate information was missing. The uncertainty of harboring the * 2, * 17, * 29 or * 31 alleles could have influenced the results from the external validation as these alleles were present in the development dataset. Patients harboring these genotypes will be falsely interpreted as fully functioning * 1 alleles. In addition, although the imputation of patients' height corrected for the influence of age, the approximation still leads to loss of data. Although the effect of patient height on the steady-state endoxifen levels is clinically irrelevant, this could have affected the validation. However, most importantly, the validation showed that the model adequately described the data despite these impediments.

In addition to developing a model using a more sensitive CYP2D6 activity scale, cut-off points which can be used for MIPD were identified. Using these cut-off values, simulations showed that the proportion of patients not reaching > 16 nM endoxifen after three months of treatment could be diminished. As endoxifen reaches steady-state concentrations after three months of tamoxifen use, using TDM guided dosing could take six to nine months to get patients on the ideal dose to reach sufficient endoxifen trough levels [8]. Using MIPD with a simple knowledge of patients' age, patient height and weight and determining CYP2D6 genotype could decrease the proportion of patients with insufficient endoxifen levels to less than 5 % when steady-state is first reached. Rapid achievement of sufficient endoxifen levels may translate into better outcomes for tumor relapse. In addition, patients with a high risk of not reaching sufficient tamoxifen steady-state concentrations can be identified before starting therapy and could be treated with an aromatase inhibitor and sooner receive adequate treatment.

However, in most cases, subsequent TDM at steady-state should still be used to identify the small amount patients that do not reach sufficient steady-state endoxifen concentrations. As shown in Fig. 4, a small proportion of patients in the 20 mg group do not reach endoxifen concentrations > 16 nM at first TDM. However, in some cases TDM does not have to be necessary, an old patient with a * 1/* 1 genotype or patients with a duplicate * 1 allele have an approximate 99 % chance of reaching adequate endoxifen concentrations at 20 mg. In addition, using MIPD, less TDM samples will be necessary as more patient will be sufficiently exposed at the first TDM occasion. When more research is performed explaining variability in tamoxifen and endoxifen pharmacokinetics, over time MIPD might wholly replace TDM.

In conclusion, applying MIPD with the developed model incorporating the influence of CYP2D6 activity on a continuous scale could diminish the amount of patients with insufficient endoxifen levels to less than 5 %. Applying MIPD may therefore improve outcomes for women with estrogen-receptor positive breast cancer. Prospective implementation of this dosing strategy will further ensure the feasibility of MIPD for tamoxifen in clinical practice.

Funding

Funding for the prospective studies are available at the original manuscripts as cited in this paper. M.S., and T.E.M. were supported in part by the Robert Bosch Stiftung (Stuttgart, Germany) and the Federal Ministry of Education and Research (BMBF; 01EK1509A), Germany. M.S was supported by the Deutsche Forschungsgemeinschaft (DFG, German Research Foundation) under Germany's Excellence Strategy—EXC 2180—390900677).

CRediT authorship contribution statement

Bram C. Agema: Conceptualization, Data curation, Formal analysis, Investigation, Methodology, Project administration, Validation, Visualization, Writing – original draft, Writing – review & editing. **Sanne M. Buijs Data curation:** Formal analysis, Investigation, Visualization, Writing – original draft, Writing – review & editing. **Sebastiaan D.T. Sassen:** Formal analysis, Investigation, Methodology, Writing – review & editing. **Thomas E. Mürdter:** Data curation, Investigation, Validation, Writing – review & editing. **Mathias Schwab:** Data curation, Investigation, Validation, Writing – review & editing. **Birgit C.P. Koch:**

Investigation, Methodology, Resources, Software, Supervision, Writing – review & editing. **Agnes Jager:** Data curation, Investigation, Writing – review & editing. **Ron H.N. van Schaik:** Data curation, Investigation, Resources, Writing – review & editing. **Ron H.J. Mathijssen:** Conceptualization, Data curation, Formal analysis, Funding acquisition, Investigation, Methodology, Resources, Supervision, Writing – review & editing. **Stijn L.W. Koolen:** Conceptualization, Data curation, Formal analysis, Investigation, Methodology, Supervision, Writing – original draft, Writing – review & editing.

Conflict of interest statement

The authors declare that they have no known competing financial interests or personal relationships that could have appeared to influence the work reported in this paper.

Data availability

For data requests, contact the original authors of the separate studies available at the original manuscripts as cited in the text.

Appendix A. Supporting information

Supplementary data associated with this article can be found in the online version at doi:10.1016/j.biopha.2023.114369.

References

[1] Early Breast Cancer Trialists' Collaborative Group, Tamoxifen for early breast cancer: an overview of the randomised trials, Lancet 351 (9114) (1998) 1451–1467.

[2] G. Early Breast Cancer Trialists' Collaborative, Effects of chemotherapy and hormonal therapy for early breast cancer on recurrence and 15-year survival: an overview of the randomised trials, Lancet 365 (9472) (2005) 1687–1717.

[3] G. Early Breast Cancer Trialists' Collaborative, C. Davies, J. Godwin, R. Gray, M. Clarke, D. Cutter, et al., Relevance of breast cancer hormone receptors and other factors to the efficacy of adjuvant tamoxifen: patient-level meta-analysis of randomised trials, Lancet 378 (9793) (2011) 771–784.

[4] L. Binkhorst, R.H. Mathijssen, A. Jager, T. van Gelder, Individualization of tamoxifen therapy: much more than just CYP2D6 genotyping, Cancer Treat. Rev. 41 (3) (2015) 289–299.

[5] E. Coezy, J.L. Borgna, H. Rochefort, Tamoxifen and metabolites in MCF7 cells: correlation between binding to estrogen receptor and inhibition of cell growth, Cancer Res. 42 (1) (1982) 317–323.

[6] L. Madlensky, L. Natarajan, S. Tchu, M. Pu, J. Mortimer, S.W. Flatt, et al., Tamoxifen metabolite concentrations, CYP2D6 genotype, and breast cancer outcomes, Clin. Pharmacol. Ther. 89 (5) (2011) 718–725.

[7] P. Saladores, T. Murdter, D. Eccles, B. Chowbay, N.K. Zgheib, S. Winter, et al., Tamoxifen metabolism predicts drug concentrations and outcome in premenopausal patients with early breast cancer, Pharmacogenomics. J. 15 (1) (2015) 84–94.

[8] C.L. Braal, A. Jager, E.O. Hoop, J.D. Westenberg, K. Lommen, P. de Bruijn, et al., Therapeutic drug monitoring of endoxifen for tamoxifen precision dosing: feasible in patients with hormone-sensitive breast cancer, Clin. Pharmacokinet. 61 (4) (2022) 527–537.

[9] L. Klopp-Schulze, A. Mueller-Schoell, P. Neven, S.L.W. Koolen, R.H.J. Mathijssen, M. Joerger, et al., Integrated data analysis of six clinical studies points toward model-informed precision dosing of tamoxifen, Front Pharmacol. 11 (2020) 283.

[10] A. Mueller-Schoell, L. Klopp-Schulze, W. Schroth, T. Murdter, R. Michelet, H. Brauch, et al., Obesity alters endoxifen plasma levels in young breast cancer patients: a pharmacometric simulation approach, Clin. Pharmacol. Ther. 108 (3) (2020) 661–670.

[11] A. Puszkiel, C. Arellano, C. Vachoux, A. Evrard, V. Le Morvan, J.C. Boyer, et al., Model-based quantification of impact of genetic polymorphisms and co-medications on pharmacokinetics of tamoxifen and six metabolites in breast cancer, Clin. Pharmacol. Ther. 109 (5) (2021) 1244–1255.

[12] R. ter Heine, L. Binkhorst, A.J. de Graan, P. de Bruijn, J.H. Beijnen, R. H. Mathijssen, et al., Population pharmacokinetic modelling to assess the impact of CYP2D6 and CYP3A metabolic phenotypes on the pharmacokinetics of tamoxifen and endoxifen, Br. J. Clin. Pharmacol. 78 (3) (2014) 572–586.

[13] W. Min, G. Yiyun, X. Haitang, Population pharmacokinetics of tamoxifen in patients with breast cancer, Chin. J. Clin. Pharmacol. Ther. 24 (4) (2019) 418–423.

[14] L. Klopp-Schulze, M. Joerger, S.G. Wicha, R. Ter Heine, C. Csajka, Z.P. Parra-Guillen, et al., Exploiting pharmacokinetic models of tamoxifen and endoxifen to identify factors causing subtherapeutic concentrations in breast cancer patients, Clin. Pharmacokinet. 57 (2) (2018) 229–242.

[15] M. van der Lee, W.G. Allard, R. Vossen, R.F. Baak-Pablo, R. Menafra, B. Deiman, et al., Toward predicting CYP2D6-mediated variable drug response from CYP2D6 gene sequencing data, Sci. Transl. Med 13 (603) (2021).

[16] L. Binkhorst, T. van Gelder, W.J. Loos, F.E. de Jongh, P. Hamberg, I. M. Moghaddam-Helmantel, et al., Effects of CYP induction by rifampicin on tamoxifen exposure, Clin. Pharmacol. Ther. 92 (1) (2012) 62–67.

[17] C.L. Braal, K. Hussaarts, L. Seuren, E. Oomen-de Hoop, P. de Bruijn, S.A.J. Buck, et al., Influence of green tea consumption on endoxifen steady-state concentration in breast cancer patients treated with tamoxifen, Breast Cancer Res. Treat. 184 (1) (2020) 107–113.

[18] K. Hussaarts, D.P. Hurkmans, E. Oomen-de Hoop, L.J. van Harten, S. Berghuis, R. J. van Alphen, et al., Impact of Curcumin (with or without Piperine) on the pharmacokinetics of Tamoxifen, Cancers 11 (3) (2019).

[19] S.A.J. Buck, C.L. Braal, M.M. Hofman, E. Oomen-de Hoop, P. de Bruijn, I. M. Ghobadi Moghaddam-Helmantel, et al., Influence of probenecid on endoxifen systemic exposure in breast cancer patients on adjuvant tamoxifen treatment, Ther. Adv. Med Oncol. 14 (2022), 17588359221081075.

[20] S.A.J. Buck, B. C.L, H. Kuijper-Tissot van Patot, L. van der Meijden-Erkelens, S.L. W. Koolen, E. Oomen-de Hoop, et al., Study on the potential pharmacokinetic interaction between cannabidiol (CBD) and tamoxifen in patients with primary breast cancer, Study Protoc. (2022).

[21] L. Binkhorst, J.S.L. Kloth, A.S. de Wit, P. de Bruijn, M.H. Lam, I. Chaves, et al., Circadian variation in tamoxifen pharmacokinetics in mice and breast cancer patients, Breast Cancer Res. Treat. 152 (1) (2015) 119–128.

[22] A.J. de Graan, S.F. Teunissen, F.Y. de Vos, W.J. Loos, R.H. van Schaik, F.E. de Jongh, et al., Dextromethorphan as a phenotyping test to predict endoxifen exposure in patients on tamoxifen treatment, J. Clin. Oncol. 29 (24) (2011) 3240–3246.

[23] L. Binkhorst, R.H. Mathijssen, I.M. Ghobadi Moghaddam-Helmantel, P. de Bruijn, T. van Gelder, E.A. Wiemer, et al., Quantification of tamoxifen and three of its phase-I metabolites in human plasma by liquid chromatography/triple-quadrupole mass spectrometry, J. Pharm. Biomed. Anal. 56 (5) (2011) 1016–1023.

[24] Consortium P.V. CYP2D6: Children's Mercy, Hospital Kansas City, 2022. ⟨https://www.pharmvar.org/gene/CYP2D6⟩. (Accessed 31 May 2022).

[25] T.E. Murdter, W. Schroth, L. Bacchus-Gerybadze, S. Winter, G. Heinkele, W. Simon, et al., Activity levels of tamoxifen metabolites at the estrogen receptor and the impact of genetic polymorphisms of phase I and II enzymes on their concentration levels in plasma, Clin. Pharmacol. Ther. 89 (5) (2011) 708–717.

[26] L.B. Sheiner, S.L. Beal, Some suggestions for measuring predictive performance, J. Pharmacokinet . Biopharm. 9 (4) (1981) 503–512.

[27] C.Y. Zhao, Z. Jiao, J.J. Mao, X.Y. Qiu, External evaluation of published population pharmacokinetic models of tacrolimus in adult renal transplant recipients, Br. J. Clin. Pharmacol. 81 (5) (2016) 891–907.

[28] N.J. Perkins, E.F. Schisterman, The inconsistency of "optimal" cutpoints obtained using two criteria based on the receiver operating characteristic curve, Am. J. Epidemiol. 163 (7) (2006) 670–675.

[29] A. Ahmad, S. Shahabuddin, S. Sheikh, P. Kale, M. Krishnappa, R.C. Rane, et al., Endoxifen, a new cornerstone of breast cancer therapy: demonstration of safety, tolerability, and systemic bioavailability in healthy human subjects, Clin. Pharmacol. Ther. 88 (6) (2010) 814–817.

[30] A. Gaedigk, S.D. Simon, R.E. Pearce, L.D. Bradford, M.J. Kennedy, J.S. Leeder, The CYP2D6 activity score: translating genotype information into a qualitative measure of phenotype, Clin. Pharmacol. Ther. 83 (2) (2008) 234–242.

[31] C. Reep, Een studie naar de lengteontwikkeling van Nederlanders, Central Bureau for Statistics, Netherlands, 2021 (Available from), ⟨https://www.cbs.nl/nl-nl/longread/statistische-trends/2021/een-studie-naar-de-lengteontwikkeling-van-nederlanders/3-resultaten⟩.

[32] E.A. Lien, E. Solheim, P.M. Ueland, Distribution of tamoxifen and its metabolites in rat and human tissues during steady-state treatment, Cancer Res. 51 (18) (1991) 4837–4844.

[33] C.L. Braal, J.D. Westenberg, S.M. Buijs, S. Abrams, T.A.M. Mulder, R.H.N. van Schaik, et al., Factors affecting inter-individual variability in endoxifen concentrations in patients with breast cancer: results from the prospective TOTAM trial, Breast Cancer Res Treat. 195 (1) (2022) 65–74.